action. The second line of coalescence observed in the $k-\epsilon$ Chien results (4 in Fig. 43) is not present in this computation. Consequently, the $k-\epsilon$ Knight model does not predict a secondary separation underneath the left side of the right vortex. The difference is due to deviation in the predictions of the pressure distribution in the spanwise direction, obtained with each turbulence model as described below.

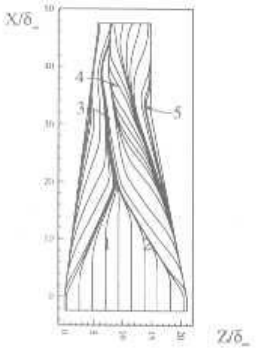

Figure 43: Computed skin friction lines $k-\epsilon$-Chien model (Case DF2)
1 Left incident separation line
2 Right incident separation line
3 Left downstream coalescence line
4 Right downstream coalescence line
5 Line of divergence (similar line near left fin)

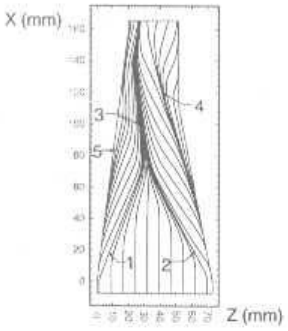

Figure 44: Computed skin friction lines $k-\epsilon$-Knight model (Case DF2)
1 Left incident separation line
2 Right incident separation line
3 Left downstream coalescence line
4,5 Lines of divergence

The surface pressure distribution in the spanwise direction at $x = 112$ mm is displayed in Figs. 46 and 47. The abscissa $z - z_{\mathrm{TML}}$ represents the spanwise distance measured from the TML (Throat Middle Line). The computations

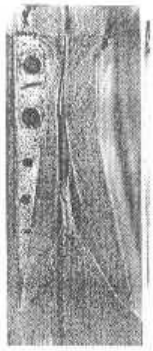

Figure 45: Experimental surface flow for $7° \times 11°$ (Case DF2)

using the $k-\epsilon$ Chien, $k-\epsilon$ Knight ("Present $k-\epsilon$"), and RSE models are in general agreement with the experiment, while the Spalart-Allmaras-Edwards, Baldwin-Lomax, and $k-\omega$ models overpredict the pressure by 16% to 21%. The $k-\epsilon$ Chien model predicts a local adverse pressure gradient in spanwise direction in the region $-10\,\mathrm{mm} < z - z_{\mathrm{TML}} < -4\,\mathrm{mm}$. Since the flow near the surface at this location is moving towards the left fin, this adverse pressure gradient causes the secondary separation and the appearance of the right downstream coalescence line (4 in Fig. 43). The $k-\epsilon$ Knight model does not predict a significant adverse pressure gradient in this region, and hence a secondary separation line does not appear.

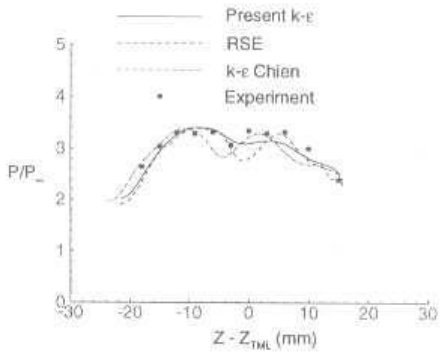

Figure 46: Wall pressure at $x = 112$ mm (Case DF2)

The surface pressure along the Throat Middle Line is displayed in Figs. 48 and 49. The computed and experimental surface pressure on TML are in good agreement for $x < 135$ mm for all models, although the computations slightly underestimate the extent of the upstream influ-